ARTICLES

Inhibition of Tumor Growth by Ribozyme-Mediated Suppression of Aberrant Epidermal Growth Factor Receptor Gene Expression

*Hitoshi Yamazaki, Hiroshi Kijima, Yasuyuki Ohnishi, Yoshiyuki Abe, Yoshiro Oshika, Takashi Tsuchida, Tetsuji Tokunaga, Atsushi Tsugu, Yoshito Ueyama, Norikazu Tamaoki, Masato Nakamura**

Background: **Amplification and rearrangement of the epidermal growth factor receptor (EGFR) gene is frequently associated with malignant gliomas. One type of EGFR mutation in primary gliomas results in overexpression of an aberrant EGFR messenger RNA (mRNA) that lacks sequences of exons II through VI of the human EGFR gene. We observed that the aberrantly spliced EGFR mRNA contains a ribozyme cleavable sequence (5′-AAG GUA AUU-3′) created by the joining of EGFR exon I to exon VII. We hypothesized that an appropriately designed ribozyme RNA could mediate site-specific cleavage of the aberrant EGFR mRNA and reduce the growth of aberrant EGFR-producing tumor cells.** ***Methods:*** **We synthesized aberrant EGFR mRNA substrates and a sequence-specific hammerhead ribozyme (abEGFR-rib) to examine the ribozyme's activity *in vitro*. We also constructed an abEGFR-rib plasmid and introduced it into ERM5–1 cells, which are murine NIH3T3 cells transfected to express an aberrant EGFR complementary DNA. We measured the growth potential of the cotransfected cells in culture and in nude mice.** ***Results:*** **The synthesized abEGFR-rib efficiently and specifically cleaved aberrant EGFR mRNA substrates *in vitro*. Expression of the transfected abEGFR-rib suppressed expression of aberrant EGFR mRNA in ERM5–1 cells and reduced the growth of tumors formed by the cotransfected cells in nude mice. Finally, the incorporation of bromodeoxyuridine, a measure of mitotic activity, was also decreased in abEGFR-rib-producing ERM5–1 cells *in vivo*.** ***Conclusion:*** **Ribozymes targeted to aberrant EGFR mRNA can inhibit the growth of tumors formed by cells that express this mRNA. [J Natl Cancer Inst 1998;90:581–7]**

The epidermal growth factor receptor (EGFR) gene encodes a Src family receptor tyrosine kinase with oncogenic potential *(1,2)*. The EGFR gene is rearranged and overexpressed in human glioblastomas *(3,4)*. Three types (I to III) of mutant EGFR genes were reported *(5)*, of which the type III mutation represents an 801 nucleotide deletion in EGFR messenger RNA (mRNA) *(6–8)*. Approximately 32% of all primary human glioblastomas with EGFR amplification have this alteration *(7)*. Furthermore, 17% of malignant gliomas possess this mutation *(9)*. Aberrant EGFR mRNA expression may be associated with carcinogenesis because NIH3T3 cells transfected with an EGFR complementary DNA (cDNA) harboring the type III mutation show transforming activity *(6)*. Recently, we detected the aberrant type III EGFR (abEGFR) transcript in proliferating glioma cells using *in situ* hybridization *(10)*. Taken together, these findings suggest that expression of aberrant EGFR mRNA plays a significant role in the continuous and aggressive growth of malignant gliomas.

Ribozymes are catalytic antisense RNAs that cleave RNA substrates in a sequence-specific manner *(11)*. The hammerhead-type ribozyme was originally discovered in satellite RNA of tobacco ringspot virus *(12,13)* and functions in that system in a *cis*-acting manner. Studies *(14,15)* showed that recombinant hammerhead-type ribozymes could also function in *trans*, with the potential for decreasing levels of specific gene transcripts. Targeted suppression of specific gene expression by ribozymes has been reported *(16,17)*, including activated ras and truncated bcr-abl genes *(18,19)*. The abEGFR mRNA contains the cleavage site sequence 5′-AAG GUA AUU-3′. Thus, the type III EGFR mRNA is cleavable at the junction of the truncated molecule (exon I spliced to exon VII) by the ribozyme. In this study, we evaluated the efficiency of ribozyme-mediated cleavage of abEGFR mRNA under different conditions *in vitro* and examined the role of ribozymes on the growth of transformed cell lines *in vivo*.

Affiliations of authors: H. Yamazaki, H. Kijima, Y. Abe, Y. Oshika, T. Tsuchida, T. Tokunaga, N. Tamaoki, M. Nakamura (Department of Pathology), A. Tsugu (Department of Neurosurgery), Tokai University School of Medicine, Bohseidai, Isehara, Kanagawa, Japan; Y. Ohnishi, Central Institute for Experimental Animals, Kawasaki, Kanagawa, Japan; Y. Ueyama, Department of Pathology, Tokai University School of Medicine, and Central Institute for Experimental Animals.

Correspondence to: Hitoshi Yamazaki, M.D., Department of Pathology, Tokai University School of Medicine, Bohseidai, Isehara-shi, Kanagawa 259-1193, Japan. E-mail: yamazaki@is.icc.u-tokai.ac.jp

See "Notes" following "References."

Materials and Methods

Ribozyme Constructs

We constructed a hammerhead ribozyme to specifically cleave abEGFR RNA in the substrate-ribozyme complex (Fig. 1, A). The DNA templates for *in vitro* transcription of the RNA substrate and the hammerhead ribozyme (Fig. 1, B and C) were synthesized by 30 cycles of the polymerase chain reaction (PCR) (denaturation at 94 °C for 90 seconds, annealing at 60 °C for 90 seconds, and extension at 72 °C for 90 seconds), using 5 U *Taq* DNA polymerase (Perkin Elmer Biosystems Division, Foster City, CA) using the following primers: (R1) 5′-TAATACGACTCACTATAGGAAAAGAAAGGTAATTA-3′ and (R2) 5′-TCACCACATAATTACCTTT-3′ for the abEGFR RNA substrate and (Rb3) 5′-TAATACGACTCACTATAGTCACCACATAATCTGATGAG-3′ and (Rb4) 5′-GAAAAGAAAGGTTTCGTCCTCACGGACTCATCAGATT-3′ for the ribozyme (abEGFR-rib). The R1 and R2 primer sequences were derived from the aberrant splice junction site connecting exons I and VII of the EGFR gene. The Rb3 and Rb4 primer sequences were derived from the hammerhead ribozyme and sequences complementary to abEGFR mRNA. A disabled hammerhead ribozyme (dis-abEGFR-rib) was also synthesized by PCR with the following primers: (Rb5) 5′-TAATACGACTCACTATAGTCACCACATAATCTAATGAG-3′ and (Rb6) 5′-GAAAAGAAAGGTTTCGTCCTCACGGACTCATTAGATT-3′. The dis-abEGFR-rib contained a single base change (G to A; Fig. 1, A) in the catalytic core compared with abEGFR-rib sequence.

Following amplification, the PCR products were fractionated through a 3% composite agarose gel (2% NuSieve, 1% Seakem) (FMC Corp., Rockland, ME), purified by DE52 (Whatman, Maidstone, U.K.) ion-exchange chromatography, and used as templates for T7 RNA polymerase (Stratagene, La Jolla, CA) catalyzed *in vitro* transcription *(20)*. For cleavage studies, the ribozymes abEGFR-rib or dis-abEGFR-rib and 25 base abEGFR substrate RNAs were labeled using [α-^{32}P]uridine triphosphate (110 TBq/mmol, Amersham Life Science Inc., Arlington Heights, IL) and T7 RNA polymerase by *in vitro* transcription according to the supplier's recommendation. The RNA substrate and ribozyme transcripts were then fractionated through TBE (i.e., 90 m*M* Tris–borate buffer [pH 8.0] and 2 m*M* EDTA) and 12% polyacrylamide gels, and the products were recovered in 1% sodium dodecyl sulfate, 0.5 *M* CH_3COONH_4, and 1 m*M* EDTA. Cleavage reactions were performed by mixing 2 pmol of abEGFR-rib or dis-abEGFR-rib RNA combined with 2 pmol of abEGFR RNA and heated at 95 °C for 2 minutes and then quickly cooled on ice. Aliquots of the ^{32}P-labeled double-stranded RNAs were added to prepare 10 μL reaction volumes. Individual reaction mixtures were incubated under different conditions (Mg^{2+} concentration: 0–40 m*M*; reaction time: 1 minute to 18 hours; RNA substrate/ribozyme molar ratio: 1–100; at 37 °C). The cleavage products were resolved on denaturing 6% TBE polyacrylamide gels and detected by autoradiography (Kodak X-OMAT AR).

Ribozyme-Producing Cells

For producing abEGFR-rib or dis-abEGFR-rib in cells, we constructed new ribozyme and disabled ribozyme DNAs by PCR and introduced them into an expression vector (pHβApr-1) *(21,22)*. Briefly, PCR was performed using the following primer pairs and each primer's partial complementary base pairing: (R25) 5′-GGAATTCAGCTGTCGACACATAATCTGATGAGTCCGTGAG-3′, (R26) 5′-GGAATTCAAGCTTAGAAAGGTTTCGTCCTCACGGACTC-3′ for abEGFR-rib and primer (R27) 5′- GGAATTCAGCTGTCGACACATAATCTAATGAGTCCGTGAG-3′, primer R26 for dis-abEGFR-rib. Following appropriate restriction endonuclease digestion, the PCR products were directionally subcloned into the *Hin*dIII and *Sal* I restriction sites of the eukaryotic expression plasmid pHβApr-1 containing a selectable hygromycin resistance gene (derived from pCEP4, Invitrogen, Leek, The Netherlands) (Fig. 2).

ERM5–1 cells were established from NIH3T3 cells by transfection with the abEGFR cDNA expression vector *(6)*. The ERM5–1 cells were maintained in Dulbecco's modified Eagle medium (DMEM; Sigma Chemical Co., St. Louis, MO) containing 6% fetal calf serum (IBL, Fujioka, Japan) and supplemented with penicillin (100 μg/ml) and streptomycin (100 μg/mL). Transfection with abEGFR-rib or dis-abEGFR-rib constructs was performed by a calcium–

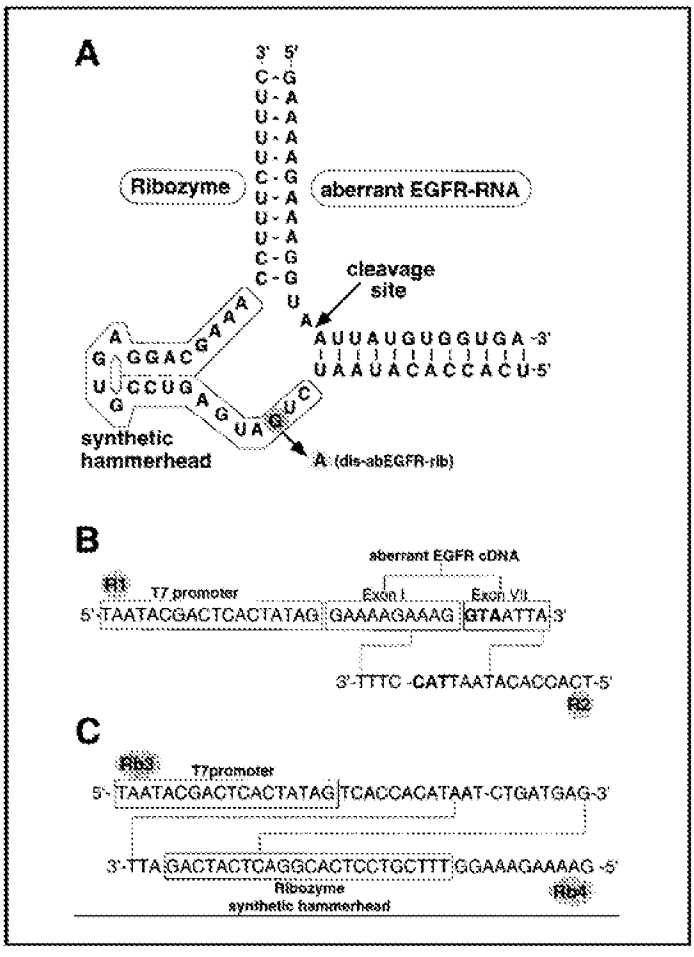

Fig. 1. Primary sequence and predicted structure of the synthetic ribozyme, substrates, and the resulting cleavage products. **A)** Schematic structure of the aberrant epidermal growth factor receptor (EGFR) substrate-ribozyme (abEGFR-rib) complex. Arrowhead indicates the cleavage site adjacent to the junction between exons I and VII present in aberrant EGFR messenger RNA (mRNA). The guanine nucleotide that was changed to adenine to create the disabled ribozyme (dis-abEGFR-rib) is highlighted. Polymerase chain reaction (PCR) primers used to synthesize aberrant EGFR mRNA. **B)** The sense primer R1 (35 mer, 5′-TAATACGACTCACTATAGGAAAAGAAAGGTAATTA-3′) includes a T7 RNA polymerase promoter sequence, and the antisense primer R2 (19 mer, 5′-TCACCACATAATTACCTTT-3′) was used for PCR-catalyzed synthesis of the truncated aberrant EGFR complementary DNA template. Regions of complementary sequence are shown by dotted lines. The 5′ boundary sequences of exon VII that form the ribozyme cleavable sequence 5′-AAGGTAATT-3′ are shown in bold letters. **C)** PCR primers used to synthesize the ribozyme. The sense primer Rb3 (38 mer, 5′-TAATACGACTCACTATAGTCACCACATAATCTGATGAG-3′) contains a T7 RNA polymerase promoter sequence and the antisense primer Rb4 (37 mer, 5′-GAAAAGAAAGGTTTCGTCCTCACGGACTCATCAGATT-3′) contains the hammerhead structure of the ribozyme abEGFR-rib. Regions of complementary sequence are shown by dotted lines.

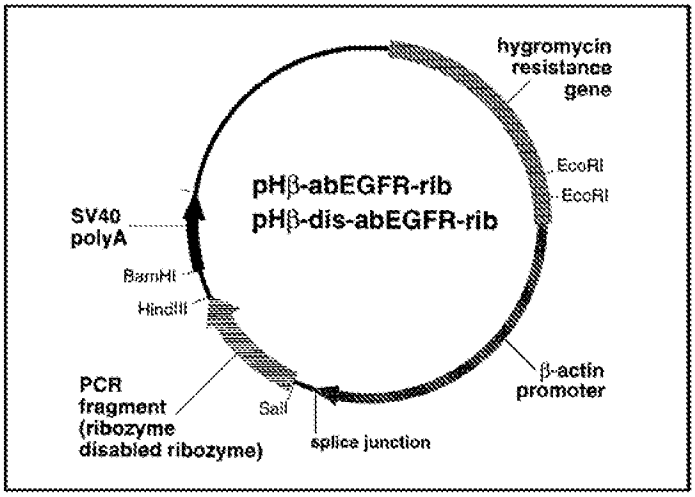

Fig. 2. Schematic representation of expression plasmids pHβ-abEGFR-rib and pHβ-dis-abEGFR-rib. The polymerase chain reaction (PCR)-generated ribozyme and disabled ribozyme DNAs (labeled "PCR fragment") were digested with *Hin*dIII and *Sal* I and ligated into *Hin*dIII/*Sal* I-digested pHβApr-1 with T4 DNA ligase. The orientation of the PCR fragment with respect to the β-actin promoter of the plasmids is shown by the arrow.

phosphate precipitation method using 10 μg of the plasmid DNA *(25)*. Plasmid-containing cells were selected in DMEM supplemented with 500 μg/mL of hygromycin for 3 weeks and subsequently isolated using a cloning cylinder.

The level of the abEGFR mRNA was determined by RNA blotting analysis. Total RNAs were extracted from ERM5–1 cells, transfected cell lines 1–21(abEGFR-rib) and 21–16(dis-abEGFR-rib), and normal human placental tissue by a single-step procedure using guanidine thiocyanate and acid phenol/chloroform *(24)*. Aliquots of 20 μg of total RNA electrophoresed through 1% agarose/6% formaldehyde gels and the RNA transfered onto nylon membranes (GeneScreen Plus; Du Pont NEN, Boston, MA). Immobilized RNAs were hybridized with ^{32}P-labeled human EGFR cDNA using standard methods and the bands visualized by autoradiography *(25)*.

Introduction of Ribozyme-Producing Cells Into Nude Mice

ERM5–1 cells, or abEGFR-rib or dis-abEGFR-rib-producing ERM5–1 cells (2 or 8×10^4 cells/mouse), were subcutaneously inoculated into nude mice (female, 8 weeks, BALB/cA-nu, Clea Japan Inc., Tokyo). The growth rates of the cells were estimated by measuring the size of the tumor lesions after inoculation. We estimated growth rates for two transfected cell lines (1-21 and 1-26) producing abEGFR-rib and two cell lines (21-12 and 21-16) producing dis-abEGFR-rib. All experiments involving laboratory animals were performed in accordance with the care and use guidelines of the Central Institute for Experimental Animals.

We estimated the fraction of growing cells by a bromodeoxyuridine (BrdU) incorporation labeling assay. Tumors were surgically removed from the mice under deep anesthesia 2 hours after intraperitoneal injection with 100 mg/kg of BrdU (Sigma Chemical Co.). Tumors were fixed in 10% formalin at room temperature for 24 hours. Sections (2–4-μm thick) from each tumor were mounted on glass slides. After blocking of endogenous peroxidase by treating the sections with 2 N HCl (30 minutes, room temperature), each preparation was incubated with 0.05% tyrosine (15 minutes, room temperature) for retrieval of BrdU antigenicity, and incubated with rat monoclonal anti-BrdU antibody (1:40, Sera-Lab, Sussex, U.K.) for 45 minutes. The sections were then incubated with horseradish peroxidase (HRP)-conjugated rabbit anti-rat immunoglobulin G 1:200, Dako, Copenhagen, Denmark) at room temperature for 30 minutes. The products were visualized by HRP reaction with 0.02% 3,3′-diaminobenzidine containing 0.005% H_2O_2. Nuclei of the cells were counterstained with hematoxylin. The number of BrdU-positive cells was determined by counting 1000 tumor cells in three different visual fields under a light microscope at a magnification of ×400.

Results

Cleavage Activity of Aberrant EGFR Ribozyme *In Vitro*

We determined the optimal conditions for RNA substrate cleavage activity by incubating abEGFR RNA and abEGFR-rib at 37 °C for 18 hours using a constant substrate/ribozyme-ratio of 1:1 and a series of Mg^{2+} concentrations (*see* "Materials and Methods" section). If the abEGFR-rib was active, we predicted that the 25-base abEGFR RNA substrate would be cleaved to produce a 13-base 5′end fragment and a 12-base 3′end fragment. Both 5′-13 base and 3′-12 base bands were visible following incubation in 1 m*M* Mg^{2+}. The intensity of the two bands increased in a concentration-dependent manner until reaching a plateau at 2 m*M* Mg^{2+} (Fig. 3, A). However dis-abEGFR-rib with a single base change in the hammerhead structure did not cleave the abEGFR RNA substrate even in the presence of 40 m*M* Mg^{2+} (Fig. 3, B).

To confirm the enzyme-like activity of the abEGFR-rib, we further characterized the ribozyme reaction. We first evaluated the time required to cleave the substrate RNA. The cleavage products were visible within 30 minutes of starting the reaction and showed a gradual increase up to 18 hours (Fig. 3, C). In fact, the substrate was almost completely exhausted after 18 hours of incubation (Fig. 3, C). Next, we examined the effect of different substrate/ribozyme ratios on ribozyme activity. The ribozyme effectively cleaved the substrate at substrate/ribozyme ratios of 2:1, 4:1, and 10:1 in the presence of 5 m*M* Mg^{2+} at 37 °C for 18 hours. No ribozyme activity was apparent at a substrate/ribozyme ratio of 100:1 (Fig. 3, D).

Effects of Ribozyme-Mediated EGFR mRNA Cleavage on Cellular Growth *In Vivo*

The expression plasmids pHβ-abEGFR-rib and pHβ-dis-abEGFR-rib were prepared (Fig. 2) and used to transfect ERM5–1 cells (*see* "Materials and Methods" section). We isolated 30 stable cell clones (1-1 to 1-30) transfected with pHβ-abEGFR-rib and 30 stable cell clones (21-1 to 21-30) transfected with pHβ-dis-abEGFR-rib after selection with 500 μg/mL hygromycin. Production of abEGFR-rib or dis-abEGFR-rib by the transfected cells was confirmed by a reverse transcriptase-coupled PCR assay (data not shown). Transfected cells had variable levels of either ribozyme. We retained two clones of each type that were the highest producers. In culture, the stable transformant 1-21, transfected with pHβ-abEGFR-rib, demonstrated reduced dendritic processing and was smaller in size compared with the pHβ-dis-abEGFR-rib transfectant 21-12 (Fig. 4, A and B). The pHβ-dis-abEGFR-rib transfectant 21-12 had a similar morphology compared with the original cell line, ERM5–1 (data not shown). Steady-state levels of the 8.1 kilobase abEGFR mRNA were decreased in the abEGFR-rib-producing cell line 1–21 compared with ERM5–1 cells (Fig. 5). In contrast, levels of abEGFR mRNA in the dis-abEGFR-rib-producing cell line, 21-16 were even greater than the levels of abEGFR mRNA detected in the ERM5–1 parent cell line (Fig. 5). Aberrant EGFR mRNA was not detected in normal human placental tissue (Fig. 5). The growth rate of the abEGFR-rib-producing cell line, 1-21, was not significantly different from that of dis-abEGFR-rib-producing cell line, 21–12, and the parent cell line, ERM5–1, under the cell culture conditions used (data not shown).

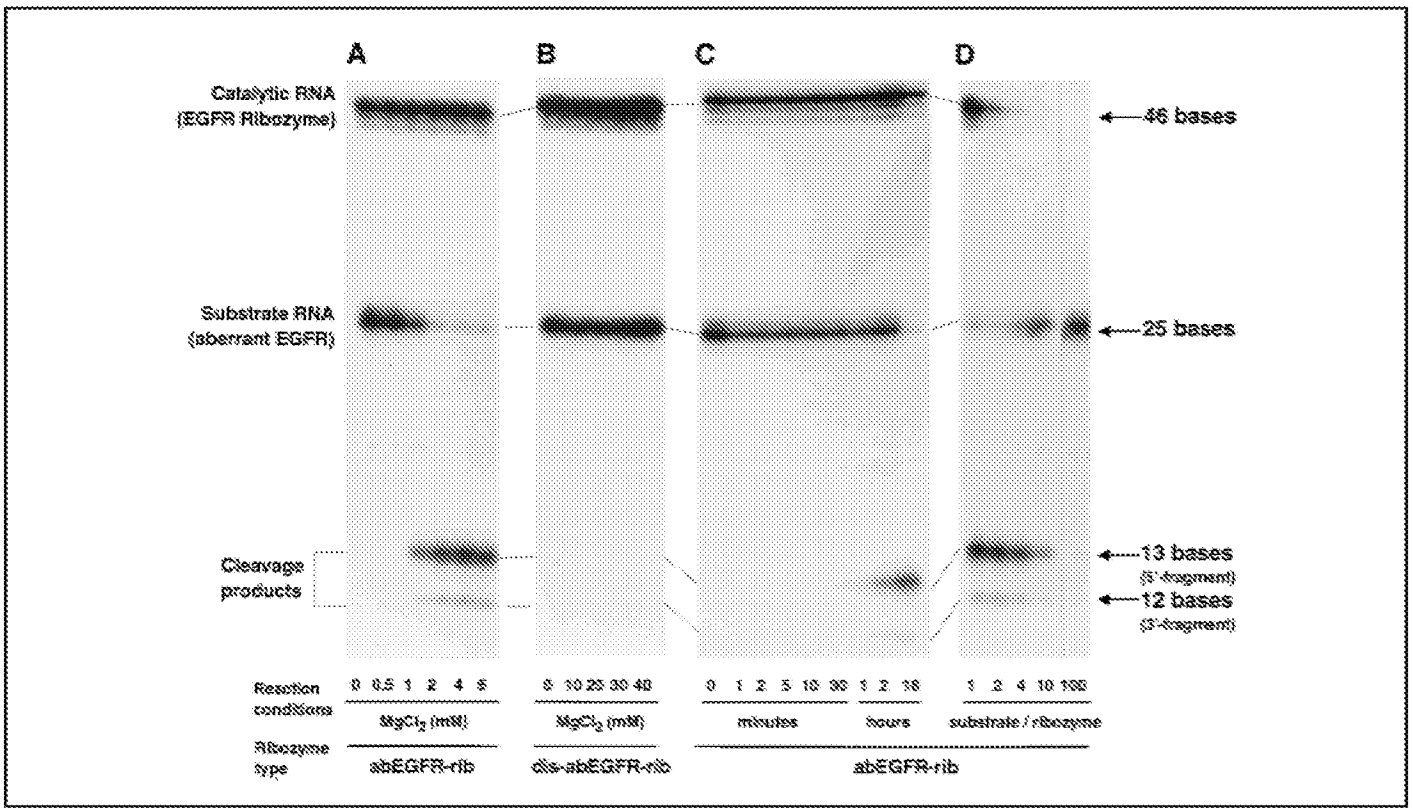

Fig. 3. *In vitro* cleavage activity using aberrant epidermal growth factor receptor (EGFR) RNA substrate. ^{32}P-labeled ribozyme(abEGFR-rib) and aberrant EGFR(abEGFR) RNA substrates were incubated using the different reaction conditions indicated at the bottom of the figure. Cleavage products were resolved from catalytic RNA and uncleaved substrate RNA by denaturing polyacrylamide gel electrophoresis. Molecular sizes of bands seen in panels A–D are indicated to the right of the figure. **A)** Cleavage activity of abEGFR-rib with the abEGFR RNA substrate in the presence of increasing concentrations of magnesium. The ribozyme and purified substrate RNAs (2 pmol each) were incubated in the presence of different concentrations of Mg^{2+} at 37 °C for 18 hours. **B)** Cleavage activity of the dis-abEGFR-rib in the presence of increasing concentration of magnesium. With exception to the $MgCl_2$ concentration, the reactions were performed as described above. **C)** Time course for RNA substrate cleavage. Cleavage reactions using the abEGFR-rib and the abEGFR RNA substrate (2 pmol each) were performed in 5 m*M* $MgCl_2$ at 37 °C. **D)** Substrate RNA cleavage activity at various ratios of the RNA substrate/ribozyme. Cleavage reactions were performed in 5 m*M* $MgCl_2$ incubated at 37 °C for 18 hours.

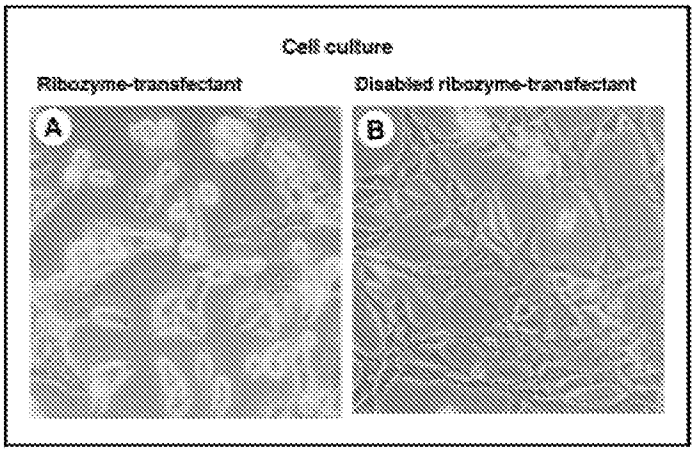

Fig. 4. Morphology of the stable ERM5–1 cell lines producing either the aberrant epidermal growth factor receptor (EGFR) ribozyme or the disabled ribozyme in culture. **A)** Phase contrast photomicrograph of cell line 1-21 transfected with the aberrant EGFR ribozyme pHβ-abEGFR-rib (×200). **B)** Cell line 21-12 transfected with the disabled ribozyme pHβ-dis-abEGFR-rib (original magnification ×200, phase contrast).

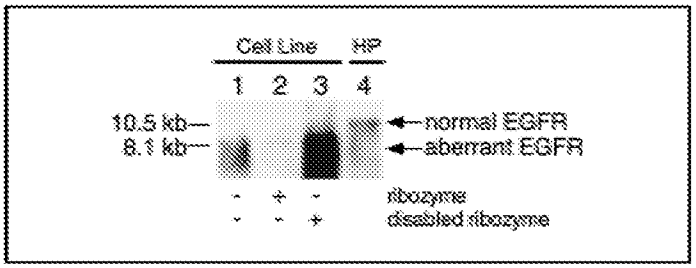

Fig. 5. Steady-state levels of aberrant epidermal growth factor receptor (EGFR) messenger RNA (mRNA) in transfected cell lines. Total RNAs were isolated from ERM5-1 cells, transfected ERM5-1 cells producing either the aberrant EGFR ribozyme (1-21 cells) or a disabled EGFR ribozyme (21-16 cells), and normal human placental tissue. Twenty micrograms total RNA were fractionated through a 1% agarose/6% formaldehyde gel and the RNA transfered to nylon membranes. The immobilized RNA was hybridized with a ^{32}P-labeled human EGFR complementary DNA *(6)* and the bands visualized by autoradiography. Molecular sizes of the normal and aberrant EGFR mRNAs are shown in kilobases (kb) to the left of the figure. Lane 1, ERM5-1 cells; lane 2, 1-21 cells; lane 3, 21-16 cells; and lane 4, human placenta.

To determine the effect of abEGFR-rib on tumor formation, the cells transfected with pHβ-abEGFR-rib (1-21 and 1-26) were inoculated into nude mice (2 or 8 × 10^4 cells/mouse). Only one tumor lesion formed with the transfected pHβ-abEGFR-rib cell line (1-26) 12 days after inoculation, whereas all of the cell lines transfected with the disabled ribozyme pHβ-dis-abEGFR-rib (21-12 and 21-16), and the ERM5–1 parent cell line formed tumors within 12 days of inoculation. By day 19, tumors had formed in four of five mice inoculated with the cell line 1-21

(Fig. 6). The tumors produced by ERM5–1 cells, abEGFR-rib cells (1-21 and 1-26), and dis-abEGFR-rib cells (21-12 and 21-16) were resected on day 19. The tumors derived from the 1-21 and 1-26 cell lines were smaller than tumors derived from the 21-12, 21-16, and ERM5-1 cell lines (Fig. 6; Table 1).

The abEGFR-rib transfectant 1-21 showed lower mitotic activity (Fig. 7, A and B). In addition, the labeling index determined by BrdU incorporation was decreased in the transfectants carrying the ribozyme expression plasmid pHβ-abEGFR-rib compared with cells carrying the disabled ribozyme expression plasmid pHβ-dis-abEGFR-rib (Table 1; Fig. 7, C and D).

Discussion

We previously reported that rearrangement of the EGFR gene frequently results in a loss of genomic DNA that leads to aberrant splicing of nucleotides 275–1075, the first and seventh exons. The resulting 801 nucleotide deletion in EGFR mRNA is associated with transforming activity and malignancy in human malignant gliomas *(6)*. We also demonstrated that the aberrant EGFR transcript was expressed in proliferating cells in malignant glioma by *in situ* hybridization *(10)*.

In this study, we prepared a hammerhead-type ribozyme based on the observation that abEGFR mRNA possesses the sequence 5′-AAG GUA AUU-3′, which is cleavable by ribozymes near the junction of exon I and exon VII in abEGFR mRNA (Figs. 1 and 2). We first used ribozymes with 9-base annealing arms *in vitro* (abEGFR-rib and dis-abEGFR-rib) to ensure substrate-specific cleavage. On the basis of our *in vitro* results, we used ribozymes with 7-base annealing arms for *in vivo* experiments (pHβ-abEGFR-rib and pHβ-dis-abEGFR-rib) in an effort to increase ribozyme turnover (binding and dissociation). The length of the homologous sequence between

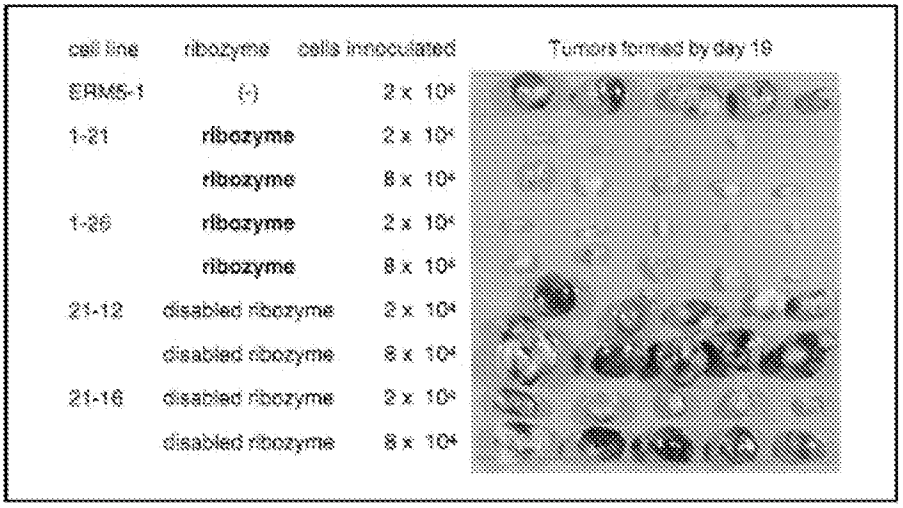

Fig. 6. Sizes of tumors resected on day 19 from nude mice following inoculation with: ERM5-1 cells; 1-21 and 1-26 cells producing aberrant EGFR ribozyme; and 21-12 and 21-16 cells producing disabled ribozyme.

Table 1. Effect of aberrant epidermal growth factor receptor (EGFR) ribozyme on tumor growth *in vivo**

			Time after tumor inoculation				
	Ribozyme	Cell line type†	Day 5	Day 10	Day 12	Day 16	Day 19
Take rate	R	1–21	0/5	0/5	0/5	1/5	4/5
	R	1–26	0/5	1/5	1/5	2/5	5/5
	D	21–12	0/5	5/5	5/5	5/5	5/5
	D	21–16	0/5	4/5	5/5	5/5	5/5
	----	ERM5–1	0/5	4/5	5/5	5/5	5/5
Tumor size, mm³	R	1–21	0	0	0	3	29 ± 40‡
	R	1–26	0	1	3	9	47 ± 53‡
	D	21–12	0	7	44	277	749 ± 254
	D	21–16	0	15	44	191	477 ± 162
	----	ERM5–1	0	12	58	289	916 ± 350
Labeling index, %	R	1–21					0.20 ± 0.10§
	R	1–26					0.30 ± 0.14§
	D	21–12					15.58 ± 1.92
	D	21–16					13.32 ± 1.23
	----	ERM5–1					15.15 ± 0.85

*Tumor nodules were grossly examined on days 5, 10, 12, and 16 at the inoculation sites. Take rate was recorded as the number of mice with tumors/total number of mice inoculated. Tumors were removed 19 days after inoculation, and each tumor was fixed for histologic analysis and for estimating the labeling index using bromodeoxyuridine incorporation. See "Materials and Methods" section for bromodeoxyuridine assay. Results obtained at day 19 after inoculation are expressed as means ± standard deviation.

†ERM5–1 cells, NIH3T3 cells stably transfected with an aberrant EGFR cDNA *(6)*, were cotransfected with a plasmid encoding the aberrant EGFR ribozyme (R) or with a plasmid encoding a disabled aberrant EGFR ribozyme (D).

‡,§Statistically significant difference comparing 21–12, 21–16, or ERM5–1 cell controls (Bonferroni/Dunn multiple comparison test, $P < .001$). Statistical analysis was performed using the SPSS program, version 6.1 for Macintosh (SPSS Inc., Chicago, IL).

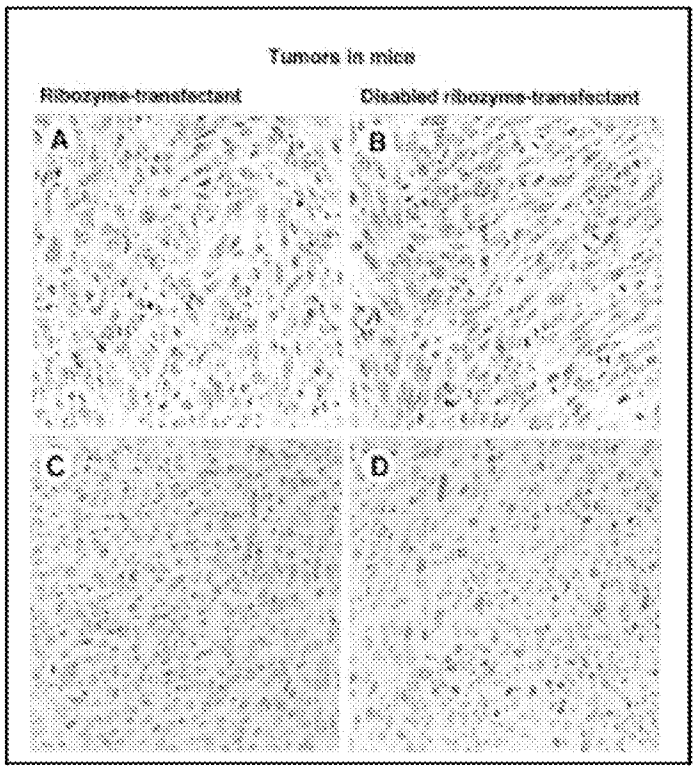

Fig. 7. Mitotic activity of tumors producing either the aberrant epidermal growth factor receptor (EGFR) ribozyme or the disabled ribozyme. **A** and **B**) stained with hematoxylin–eosin only, original magnification ×390. **A**) Transfectant 1-21 producing ribozyme abEGFR-rib. **B**) Transfectant 21-12 producing disabled ribozyme dis-abEGFR-rib, showing numerous mitotic figures. **C**) Transfectant 1-21 producing ribozyme abEGFR-rib, with a few cells faintly labeled with bromodeoxyuridine (BrdU). **D**) Transfectant 21-12 producing disabled ribozyme dis-abEGFR-rib, with numerous cells labeled with BrdU. Cells in panels C and D are counterstained with hematoxylin, original magnification ×130. *See* "Materials and Methods" section for the BrdU assay.

abEGFR-rib and its target RNA was adequate for cleavage of the RNA target *in vitro*. The ribozyme effectively cleaved the substrate even at low Mg^{2+} concentrations (1 m*M*). Although the physiologic intracellular Mg^{2+} concentration is in the range of 0.2–1.0 m*M* *(26)*, we predicted that the ribozyme would be effective in cleaving abEGFR RNA by using some other divalent cations *in vivo*. As expected, a disabled ribozyme (dis-abEGFR-rib) did not cleave the substrate RNA molecule, even at Mg^{2+} concentrations as high as 40 m*M*. These results suggest that the cleavage activity mediated by abEGFR-rib was a ribozyme-specific catalytic reaction rather than a simple antisense-neutralizing reaction *in vitro*. The cleavage products were detected within 30 minutes of commencement of the reaction and showed a marked increase within 2 hours (Fig. 3, A). The greater time required for the cleavage reaction by abEGFR-rib suggested that the speed of dissociation of the ribozyme from its reaction complex may be slow compared with proteinaceous enzymes, and that this may represent the rate-limiting step for the cleavage reaction. The abEGFR-rib was effective at a substrate/ribozyme ratio of 4:1 in the presence of 5 m*M* Mg^{2+} at 37 °C for 18 hours. The ribozyme retained its activity, even at a substrate/ribozyme ratio of 10:1 (Fig. 3, D). Taken together, these results suggest that the abEGFR-rib acts as an enzyme-like catalytic molecule *in vitro*.

When abEGFR-rib-producing ERM5–1 cells were inoculated into nude mice, the introduced cells still formed tumors. However, these tumors were at least one tenth the size of tumors produced by the original ERM5–1 cells or dis-abEGFR-rib-producing cells (Table 1). The mitotic activity was also decreased in the abEGFR-rib-producing cell lines. Thus, we confirmed the inhibitory effect of abEGFR-rib on the growth of transformed cells *in vivo*.

The aberrant EGFR molecule in glioblastomas retains the transmembrane domain and is actually functional as a cell-surface receptor *(6)*. Most likely, the first exon still encodes the leader sequence of the aberrant EGFR. It is plausible that the mRNA cleaved by the abEGFR-rib may be translated from the next in-frame "ATG" codon (theoretically, Met 318 in the full-length cDNA) to generate a new protein product. This putative new protein is predicted to retain functional domains for signal transduction, although it would not have a leader sequence capable of spanning the cellular membrane. Thus, the protein's intracellular localization may affect signal transduction in relation to cell growth.

On the basis of our results, we conclude that the aberrant EGFR mRNA-specific hammerhead ribozyme described here effectively inhibits cellular growth. Because this deletion in EGFR mRNA is known to be closely associated with malignant gliomas, we think that the ribozyme-mediated specific cleavage of aberrant EGFR transcripts is an elegant approach leading to gene therapy of malignant glioma.

References

(1) Downward J, Yarden Y, Mayes E, Scrace G, Totty N, Stockwell P, et al. Close similarity of epidermal growth factor receptor and v-erb-B oncogene protein sequences. Nature 1984;307:521–7.

(2) Yamamoto T, Nishida T, Miyajima N, Kawai S, Ooi T, Toyoshima K. The erbB gene of avian erythroblastosis virus is a member of the src gene family. Cell 1983;35:71–8.

(3) Yamazaki H, Fukui Y, Ueyama Y, Tamaoki N, Kawamoto T, Taniguchi S, et al. Amplification of the structurally and functionally altered epidermal growth factor receptor gene (c-erbB) in human brain tumors. Mol Cell Biol 1988;8:1816–20.

(4) Nishikawa R, Ji RC, Harmon XD, Lazar CS, Gill GN, Cavenee WK, et al. A mutant epidermal growth factor receptor common in human glioma confers enhanced tumorigenicity. Proc Natl Acad Sci U S A 1994;91:7727–31.

(5) Wong AJ, Ruppert JM, Bigner SH, Grzeschik CH, Humphrey PA, Bigner DS, et al. Structural alterations of the epidermal growth factor receptor gene in human gliomas. Proc Natl Acad Sci U S A 1992;89:2965–9.

(6) Yamazaki H, Ohba Y, Tamaoki N, Shibuya M. A deletion mutation within the ligand binding domain is responsible for activation of epidermal growth factor receptor gene in human brain tumors. Jpn J Cancer Res 1990;81:773–9.

(7) Sugawa N, Ekstrand AJ, James CD, Collins VP. Identical splicing of aberrant epidermal growth factor receptor transcripts from amplified rearranged genes in human glioblastomas. Proc Natl Acad Sci U S A 1990;87:8602–6.

(8) Ekstrand AJ, Sugawa N, James CD, Collins VP. Amplified and rearranged epidermal growth factor receptor genes in human glioblastomas reveal deletions of sequences encoding portions of the N-and/or C-terminal tails. Proc Natl Acad Sci U S A 1992;89:4309–13.

(9) Humphrey PA, Wong AJ, Vogelstein B, Zalutsky MR, Fuller GN, Archer GE, et al. Anti-synthetic peptide antibody reacting at the fusion junction of deletion-mutant epidermal growth factor receptors in human glioblastoma. Proc Natl Acad Sci U S A 1990;87:4207–11.

(10) Tsugu A, Kijima H, Yamazaki H, Ohnishi Y, Takamiya Y, Abe Y, et al. Localization of aberrant messenger RNA of epidermal growth factor receptor (EGFR) in malignant glioma. Anticancer Res 1997;17:2225–32.

(11) Cech TR, Zaug AJ, Grabowski PJ. *In vitro* splicing of the ribosomal RNA precursor of Tetrahymena: involvement of a guanosine nucleotide in the excision of the intervening sequence. Cell 1981;27(3 Pt 2):487–96.
(12) Buzayan JM, Gerlach WL, Bruening G. Non-enzymatic cleavage and ligation of RNAs complementary to a plant virus satellite RNA. Nature 1986;323:349–53.
(13) Prody GA, Bakos JT, Buzayan JM, Schneider R, Bruening G. Autolytic processing of dimeric plant virus satellite RNA. Science 1986;231:1577–80.
(14) Uhlenbeck OC. A small catalytic oligoribonucleotide. Nature 1987;328:596–600.
(15) Haseloff J, Gerlach WL. Simple RNA enzymes with new and highly specific endoribonuclease activities. Nature 1988;334:585–91.
(16) Sarver N, Cantin EM, Chang PS, Zaia JA, Ladne PA, Stephens DA, et al. Ribozymes as potential anti-HIV-1 therapeutic agents. Science 1990;247:1222–5.
(17) Ohkawa J, Yuyama N, Takabe Y, Nishikawa S, Taira K. Importance of independence in ribozyme reactions: kinetic behavior of trimmed and of simply connected multiple ribozymes with potential activity against human immunodeficiency virus. Proc Natl Acad Sci U S A 1993;90:11302–6.
(18) Ohta Y, Kijima H, Ohkawa T, Kashani-Sabet M, Scanlon KJ. Tissue-specific expression of an anti-ras ribozyme inhibits proliferation of human malignant melanoma cells. Nucleic Acids Res 1996;24:938–42.
(19) Snyder DS, Wu Y, Wang JL, Rossi JJ, Swiderski P, Kaplan BE, et al. Ribozyme-mediated inhibition of bcr-abl gene expression in a Philadelphia chromosome-positive cell line. Blood 1993;82:600–5.
(20) Davanloo P, Rosenberg AH, Dunn JJ, Studier FW. Cloning and expression of the gene for bacteriophage T7 RNA polymerase. Proc Natl Acad Sci U S A 1984;81:2035–9.
(21) Gunning P, Leavitt J, Muscat G, Ng SY, Kedes L. A human β-actin expression vector system directs high-level accumulation of antisense transcripts. Proc Natl Acad Sci U S A 1987;84:4831–5.
(22) Ng SY, Gunning P, Eddy R, Ponte P, Leavitt J, Show T, et al. Evolution of the functional human β-actin gene and its multi-pseudogene family: conservation of noncoding regions and chromosomal dispersion of pseudogenes. Mol Cell Biol 1985;5:2720–32.
(23) Chen C, Okayama H. High-efficiency transformation of mammalian cells by plasmid DNA. Mol Cell Biol 1987;7:2745–52.
(24) Chomczynski P, Sacchi N. Single-step method of RNA isolation by acid guanidinium thiocyanate-phenol-chloroform extraction. Anal Biochem 1987;162:156–9.
(25) Feinberg AP, Vogelstein B. A technique for radiolabeling DNA-restriction endonuclease fragments to high specific activity. Anal Biochem 1983;132:6–13.
(26) Dirks JH, Alfrey AC. Normal and abnormal magnesium metabolism. In: Schrier RW, editor. Renal and electrolyte disorders. 3rd ed. Boston: Little, Brown, 1986:331–59.

Notes

Supported by a Grant-in-Aid for Cancer and Scientific Research from the Ministry of Education, Science and Culture of Japan (Y. Ueyama; 05670210), and by 1994 Tokai University School of Medicine Research Aid.

We thank Mr. Y. Tada, Ms. K. Murata, and Mr. J. Ito for their skillful technical assistance.

Manuscript received October 27, 1997; revised January 27, 1998; accepted February 12, 1998.

Middle T antigen-transformed endothelial cells exhibit an increased activity of nitric oxide synthase. J Exp Med 1995;181:9–19.
(24) Weidner N, Semple JP, Welch WR, Folkman J. Tumor angiogenesis and metastasis—correlation in invasive breast carcinoma. N Engl J Med 1991; 324:1–8.
(25) Ziche M, Gullino PM. Angiogenesis and neoplastic progression *in vitro*. J Natl Cancer Inst 1982;69:483–7.
(26) Ziche M, Alessandri G, Gullino PM. Gangliosides promote the angiogenic response. Lab Invest 1989;61:629–34.
(27) Ziche M, Morbidelli L, Masini E, Amerini S, Granger HJ, Maggi CA, et al. Nitric oxide mediates angiogenesis *in vivo* and endothelial cell growth and migration *in vitro* promoted by substance P. J Clin Invest 1994;94: 2036–44.
(28) Chomczynski P, Sacchi N. Single-step method of RNA isolation by acid guanidinium thiocyanate-phenol-chloroform extraction. Anal Biochem 1987;162:156–9.
(29) Ziche M, Parenti A, Ledda F, Dell'Era P, Granger HJ, Maggi CA, et al. Nitric oxide promotes proliferation and plasminogen activator production by coronary venular endothelium through endogenous bFGF. Circ Res 1997;80:845–52.
(30) Reiling N, Ulmer AJ, Duchrow M, Ernst M, Flad HD, Hauschildt S. Nitric oxide synthase: mRNA expression of different isoforms in human monocytes/macrophages. Eur J Immunol 1994;24:1941–4.
(31) Ignarro LJ. Signal transduction mechanisms involving nitric oxide. Biochem Pharmacol 1991;41:485–90.
(32) Franchi A, Gallo O, Boddi V, Santucci M. Prediction of occult neck metastases in laryngeal carcinoma: role of proliferating cell nuclear antigen, MIB-1, and E-cadherin immunohistochemical determination. Clin Cancer Res 1996;2:1801–8.
(33) Cobbs CS, Brenman JE, Aldape KD, Bredt DS, Israel MA. Expression of nitric oxide synthase in human central nervous system tumors. Cancer Res 1995;55:727–30.
(34) Villiotou V, Deliconstantinos G. Nitric oxide, peroxynitrite and nitrosocompounds formation by ultraviolet A (UVA) irradiated human squamous cell carcinoma: potential role of nitric oxide in cancer prognosis. Anticancer Res 1995;15:931–42.
(35) Jenkins DC, Charles IG, Baylis SA, Lelchuk R, Radomski MW, Moncada S. Human colon cancer cell lines show a diverse pattern of nitric oxide synthase gene and nitric oxide generation. Br J Cancer 1994;70: 847–9.
(36) Green SJ. Nitric oxide in mucosal immunity [published erratum appears in Nat Med 1995;1:717]. Nat Med 1995;1:515–7.
(37) Guo FH, De Raeve HR, Rice TW, Stuehr DJ, Thunnissen FB, Erzurum SC. Continuous nitric oxide synthesis by inducible nitric oxide synthase in normal human airway epithelium *in vivo*. Proc Natl Acad Sci U S A 1995; 92:7809–13.
(38) Heppner GH. Tumor heterogeneity. Cancer Res 1984;44:2259–65.
(39) Dunstan S, Powe DG, Wilkinson M, Pearson J, Hewitt RE. The tumour stroma of oral squamous cell carcinomas show increased vascularity compared with adjacent host tissue. Br J Cancer 1997;75:559–65.
(40) Andrade SP, Hart IR, Piper PJ. Inhibitors of nitric oxide synthase selectively reduce flow in tumor-associated neovasculature. Br J Pharmacol 1992;107:1092–5.
(41) Tozer GM, Prise VE, Chaplin DJ. Inhibition of nitric oxide synthase induces a selective reduction in tumor blood flow that is reversible with L-arginine. Cancer Res 1997;57:948–55.
(42) Vamvakas S, Schmidt HH. Just say NO to cancer? [editorial]. J Natl Cancer Inst 1997;89:406–7.
(43) Takahashi M, Fukuda K, Ohata T, Sugimura T, Wakabayashi K. Increased expression of inducible and endothelial constitutive nitric oxide synthases in rat colon tumors induced by azoxymethane. Cancer Res 1997;57: 1233–7.
(44) Xie K, Huang S, Dong Z, Juang SH, Wang Y, Fidler IJ. Destruction of bystander cells by tumor cells transfected with inducible nitric oxide (NO) synthase gene. J Natl Cancer Inst 1997;89:421–7.
(45) Forrester K, Ambs S, Lupold SE, Kapust RB, Spillare EA, Weinberg WC, et al. Nitric oxide-induced p53 accumulation and regulation of inducible nitric oxide synthase expression by wild-type p53. Proc Natl Acad Sci U S A 1996;93:2442–7.
(46) Dameron KM, Volpert OV, Tainsky MA, Bouck N. Control of angiogenesis in fibroblasts by p53 regulation of thrombospondin-1. Science 1994; 265:1582–4.
(47) Gallo O, Chiarelli I, Bianchi S, Calzolari A, Porfirio B. Loss of the p53 mutation after irradiation is associated with increased aggressiveness in recurred head and neck cancer. Clin Cancer Res 1996;2:1577–83.
(48) Tsurumi Y, Murohara T, Krasinski K, Chen D, Witzenbichler B, Kearney M, et al. Reciprocal relation between VEGF and NO in the regulation of endothelial integrity. Nat Med 1997;3:879–86.
(49) Sauter E, Nesbit M, Herlyn M. Vascular endothelial growth factor (VEGF) is a marker of disease progression in head and neck cancer [abstract]. Proc Am Assoc Cancer Res 1997;38:331.
(50) Inoue K, Ozeki Y, Saganuma T, Sugiura Y, Tanaka S. Vascular endothelial growth factor expression in primary esophageal squamous cell carcinoma. Association with angiogenesis and tumor progression. Cancer 1997; 79: 206–13.
(51) Parenti A, Morbidelli L, Cui XL, Douglas JG, Hood JD, Granger HJ, et al. Nitric oxide is an upstream signal of vascular endothelial growth factor-induced extracellular signal-regulated kinase$_{1/2}$ activation in postcapillary endothelium. J Biol Chem 1998;273:4220–6.

Notes

O. Gallo and E. Masini contributed equally to this work.

Supported by funds from the Italian Association for Cancer Research (Special Project "Angiogenesis") (M. Ziche), European Communities BIOMED-2("Angiogenesis and Cancer") (M. Ziche), the National Council of Research (M. Ziche and E. Masini), and the Italian Ministry of University, Scientific and Technological Research (M. Ziche).

We thank Professor D. Bani, University of Florence, for conducting the immunofluorescence analysis and Professor V. Boddi, University of Florence, for doing the statistical evaluation.

Manuscript received October 30, 1997; revised February 10, 1998, accepted February 13, 1998.